Self-Assembling MEMS Variable and Fixed RF Inductors

Victor M. Lubecke, *Senior Member, IEEE*, Bradley Barber, *Member, IEEE*, Edward Chan, Daniel Lopez, Mihal E. Gross, and Peter Gammel, *Member, IEEE*

***Abstract*—Inductors play a key role in wireless front-end circuitry, yet are not generally well suited for conventional RF integrated-circuit (RFIC) fabrication processes. We have developed inductors that can be fabricated on a conventional RFIC silicon substrate, which use warping members to assemble themselves away from the substrate to improve quality factor (Q) and self-resonance frequency (SRF), and to provide a degree of variation in inductance value. These self-assembling variable inductors are realized through foundry provided microelectromechanical systems (MEMS) processing and have demonstrated temperature stable Q values greater than 13, SRF values well above 15 GHz, and inductance variations greater than 18%. Simulations suggest the potential for Q values above 20 and inductance variations greater than 30%, with optimized processing.**

***Index Terms*—Inductor, MEMS, micromachining, RFIC, variable.**

I. Introduction

CURRENT interest in high-performance personal wireless transceivers, such as miniature mobile phones and *connected* personal data assistants (PDAs), has created a strong demand for extremely compact and power-efficient radio circuitry. While the size, performance, and cost benefits of integration technology has been widely exploited in baseband circuitry for these products, RF front-end circuitry has remained heavily dependent on large discrete passive components, such as inductors. Inductors play a key role in resonators for low phase-noise voltage-controlled oscillators (VCOs) and as filter components and reactive impedance matching elements in other low-noise RF circuits. Variable inductors can provide the benefit of performance optimization and added functionality to RF front-end circuitry. For these applications, inductors must be accurate and operate with low losses, low power consumption, and high linearity. Inductors with quality factors (Q's) greater than 15, self-resonance frequencies above 10 GHz, and accuracies better than $+/-2\%$ are generally desired for RF integrated-circuit (RFIC) applications [1], while even a small degree of continuous inductance variation can be useful for finely tuning the frequency of resonant circuits or accurately matching impedances. However, planar inductors integrated directly with RFIC technology are subject to extreme parasitic losses resulting from their large flat geometry coupling to the low-resistivity substrate. Loss-reduction techniques such as local substrate removal and three-dimensional (3-D) construction can help, but not without imposing fabrication and compatibility issues [2], [3]. Inductance variation techniques through active circuitry or switches also introduce performance and fabrication compromises that limit their appeal [4], [5].

We have developed integrated RF inductors that can provide reduced parasitic losses and variable inductance. They are based on a 3-D self-assembling structure that uses interlayer stress to bend itself out of the plane in which it is fabricated. The structure separates itself from the circuit substrate to minimize parasitic losses and uses thermally controlled inter-member positioning to alter the overall inductance. The fabrication process is conventional for micromachines and consistent with current preprocess CMOS circuit integration techniques [6]. The structures are resilient and repeatable. Metal-limited temperature stable Q values greater than 13 have been demonstrated, as well as continuous inductance variations greater than 18%, with a potential for Q values greater than 20 and inductance variations greater than 30%.

II. Design and Fabrication

When placed on a low-resistivity substrate, planar inductor geometries present both a desired inductance and a parasitic capacitance. Reducing the size of the conducting elements brings about a reduction in parasitic capacitance, but also increases the resistive loss. The approach presented here for improving this situation involves lifting the structure off the substrate plane to reduce the capacitance without increasing the resistance. The inductors assemble by means of an interlayer stress that causes portions of the inductor to bend away from the substrate in a controllable manner. The simplest means for doing this is to fabricate the inductor in the substrate plane over a sacrificial layer, with anchor points at both ends connecting through to the substrate. By using two or more material layers deposited with different stresses, the inductor can be made to curl away from the substrate when the sacrificial layer is removed [1]. This type of deformation has been observed for large surface-micromachined structures, resulting from residual tensile stress between polysilicon and Cr–Au metal layers (with radius of curvature on the order of 1–2 mm) [7]. While initially considered undesirable, the effect has been used to great advantage for methods

Manuscript received February 28, 2001. This work was supported by Lucent Technologies.

V. M. Lubecke is with Bell Laboratories, Lucent Technologies, Murray Hill, NJ 07974 USA (e-mail: lubecke@ lucent.com).

B. Barber, D. Lopez, M. E. Gross, and P. Gammel were with Bell Laboratories, Lucent Technologies, Murray Hill, NJ 07974 USA. They are now with Agere Systems (formerly the Microelectronics Group, Lucent Technologies), Murray Hill, NJ 07974 USA.

E. Chan was with the Bell Laboratories, Lucent Technologies, Murray Hill, NJ 07974 USA. He is now with DigiLens Inc., Sunnyvale, CA 94085 USA.

Publisher Item Identifier S 0018-9480(01)09394-2.

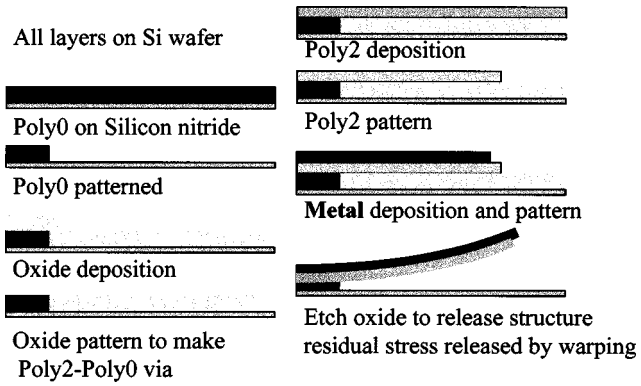

Fig. 1. Simplified fabrication for self-assembling inductors. The interlayer stress between the metal and polysilicon layers causes the patterned inductor to curl up off the substrate upon release.

of device self-assembly upon release [8]. The basic application of this technique to the fabrication of a simple inductor is illustrated in Fig. 1.

Fabrication of the inductors described here was performed through thin-film photolithographic techniques. The structures were formed as a Cr–Au layer (0.5 μm) over a polysilicon layer (1.5 μm), patterned on a sacrificial oxide layer (2 μm) over the substrate, with a final etch-release/self-assembly step to achieve the desired 3-D structures. Fabrication was carried out using the Cronos multi-user microelectromechanical process (MUMPS) [9]. While suitable for demonstrating the inductor concept, the MUMPS process imposes unnecessary limits on inductor performance. Specifically, the substrate has higher conductivity (1 $\Omega \cdot$ cm) than needed for an RFIC (about 10 $\Omega \cdot$ cm), which reduces Q, and the metal layer is too thin to minimize ohmic losses at RF/microwave frequencies (less than one skin depth). Another significant limitation is that the single metal layer in this process limits inductance to low values by restricting designs to a single turn (no bridge layer). Also, the finite resistance of the polysilicon mechanical support adds a parasitic conductance in parallel with the inductor. The process, however, is convenient, widely used, and allows for the demonstration of an effective technique for fabricating microelectromechanical (MEMS)-first integrated RF inductors, while remaining extendible to a more optimal custom process. It also provides a reasonable representation of RFIC demands and the basic features of promising embedded MEMS approaches [7]. A scanning electron microscopy (SEM) photograph of one such self-assembled inductor design is shown in Fig. 2(a). The triangular shaped inductor shown is about 1200 μm in length, with anchor pads spaced with a pitch of 150 μm.

A high-Q variable inductor can be similarly formed by creating a structure that remains sufficiently above the substrate at all operating temperatures, yet incorporates mutually coupled current-carrying members that move with respect to each other as temperature varies, thus affecting the mutual component of the total inductance. The temperature variations needed to actuate such a structure can be environmental or localized joule heating effects induced by an applied dc current. One such variable inductor is shown in Fig. 3(a). The inductor consists of two loops that assemble themselves above the substrate, with a relative angle between them that can be thermally con-

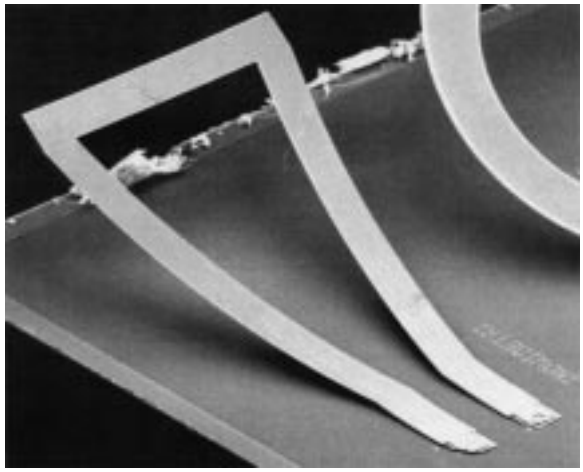

(a)

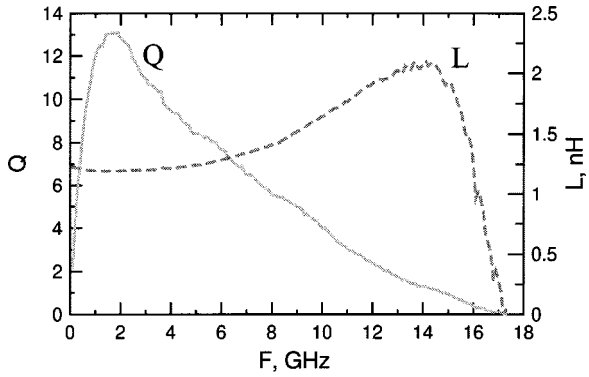

(b)

Fig. 2. Triangular self-assembling inductor. (a) SEM photograph shows inductor curling away from the substrate resulting in very good (b) Q and SRF.

trolled. The differential motion results from a cross-member corrugation structure in the inner loop that causes it to bend with temperature at a different rate than the outer loop [10]. Other such mechanisms, such as anchor hooks, have also been demonstrated. The hairpin-shaped conductors were roughly 50-μm wide, separated by a 25-μm gap, and the longer loop was about 1200-μm long. The pitch between anchor pads was 150 μm.

The simple form of these inductors allows improved electrical performance, with high yield potential and good mechanical integrity. The structures are thin and flexible, yet quite resilient and can be pushed flat to the substrate and still return to their assembled position unaffected. While structurally necessary, the anchor pads for such inductors present an unwanted capacitance that needs to be minimized without compromising mechanical stability. Several pad variations were examined, with better electrical performance obtained for pads with an entombed layer of oxide [1] or contact area minimized. An alternative more complex design that does not require large anchor pads can be realized through the same fabrication process. A hairpin-shaped example of such an inductor is shown in Fig. 4(a). The inductor is attached to the substrate by hinges rather than anchor pads, and ratchet-locked curling elements are used to assemble the inductor into a semivertical position that holds fast when shaken and changes very little with subsequent temperature changes. The hinges can be further fixed in place by electro-

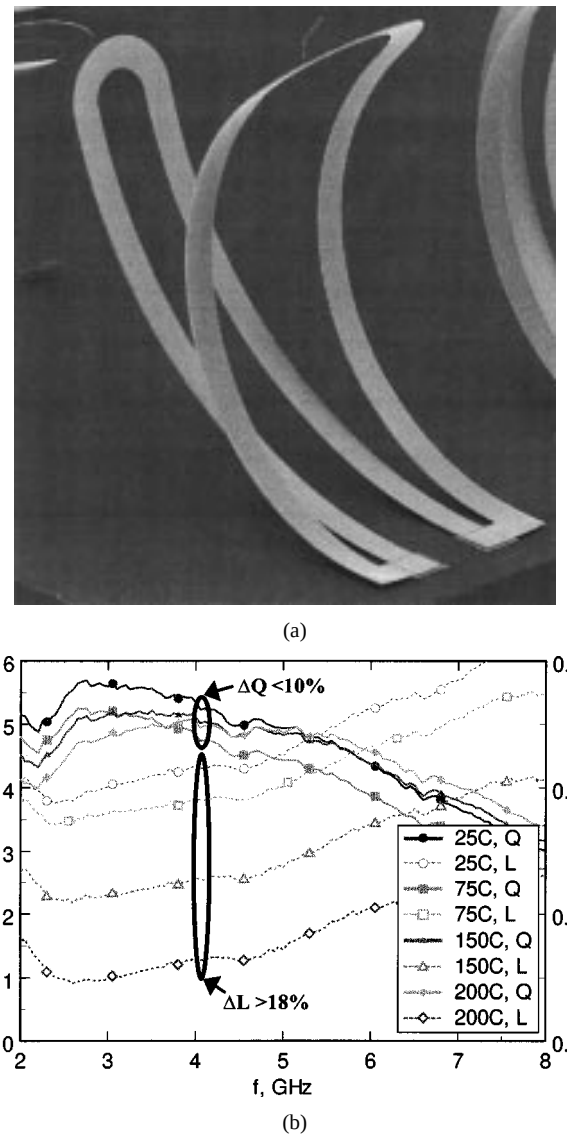

Fig. 3. Variable self-assembling hairpin inductor. (a) SEM photograph shows two loops with different corrugations, which bend with (b) temperature at different rates to allow the mutual inductance to be varied.

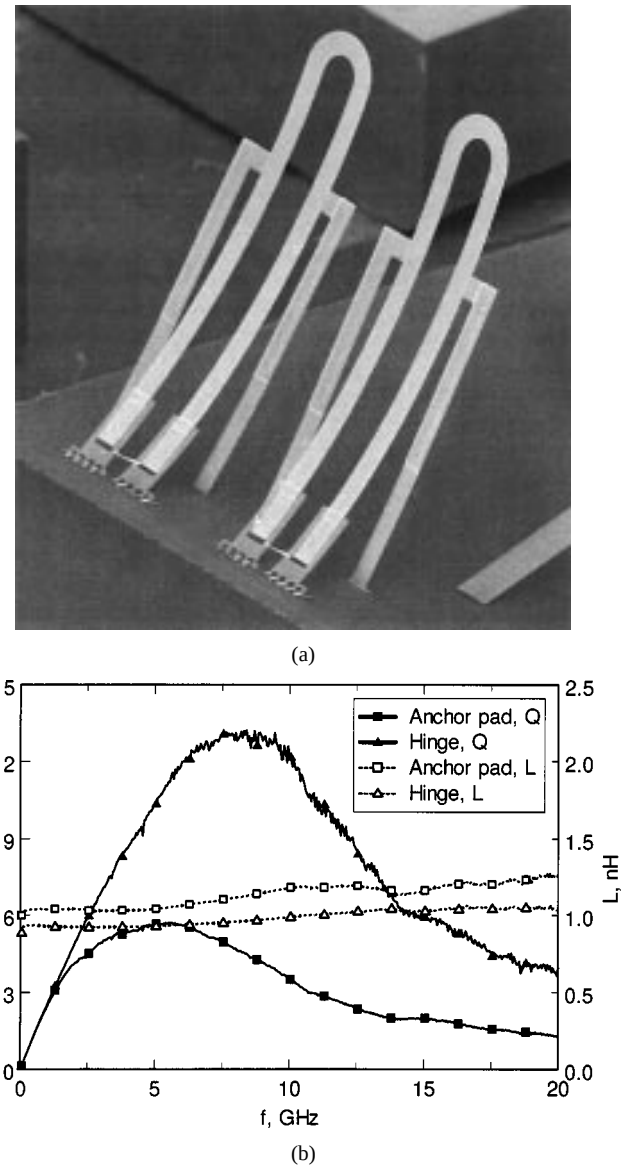

Fig. 4. Hinged self-assembling hairpin inductor. (a) SEM photograph shows steep slope of hinged structure with warped supports, which significantly improves (b) high-frequency Q.

plating the structure, which can also create a dependable ohmic connection to a circuit and reduce ohmic loss. An added benefit for this design is increased angle with which the inductor rises from the substrate, which significantly reduces parasitic capacitance. The conductors were about 50-μm wide and the loops about 1200-μm long. The pitch between attachment points was 150 μm.

III. Performance and Analysis

Various self-assembling inductors were fabricated and their scattering parameters measured using a Cascade-Microtech Microchamber probe station with ambient temperature control and an HP 8510B network analyzer. The performance for the described triangular fixed-value inductor is shown in Fig. 2(b). Measurements were made at room temperature for frequencies up to 18 GHz. The peak value of Q at the design frequency was about 13 and the self-resonance frequency (SRF) occurred at about 17 GHz, both very suitable for high-performance RFICs. Here, Q is defined as the ratio of the imaginary part of the measured impedance divided by the real part, and inductance (L) as the imaginary part of the measured impedance divided by the angular frequency. Note that the metal layer for this inductor was thinner than optimal (about 1.5 μm) and the effect of the anchor pads (an essential part of the inductor) was not deembedded.

Various other measurements were made for this type of self-assembled inductor to better determine the benefits and limitations. A hairpin-shaped inductor was made with a hook at its end to clearly isolate the effect of release on inductance and Q. With the inductor released, but hooked flat to the substrate, its Q and inductance remained as before release. Unhooked, the peak Q jumped from just under four to just over six and remained consistently higher than the flat inductor at increasing frequency. The in-band inductance remained at about 1 nH, but with the SRF extended from below 10 to above 15 GHz. To assess repeatability, five copies of one such inductor were

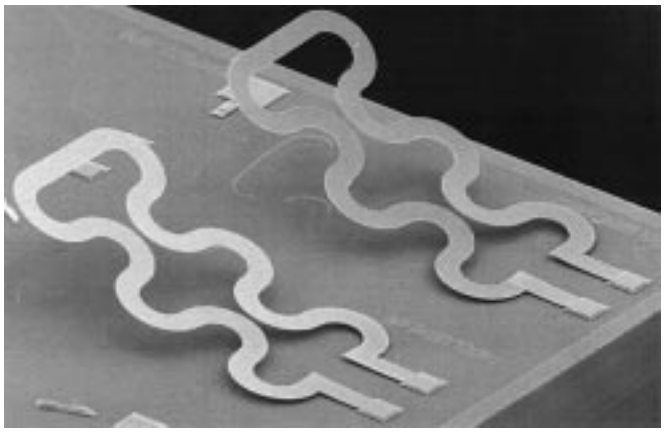

Fig. 5. Thicker metal effects on meander inductors. The additional height of the inductor in the background in this SEM photograph resulted from the added interlayer stress from its thicker metal.

fabricated on different CRONOS wafers, with a resulting variation in inductance of 1%–2% around 2 GHz and an SRF variation of about 5%. Values of Q were similarly consistent. Metal effects were also investigated by measuring two like inductors differing only by the thickness of the metal layer. Some MUMPS processing runs allow a second layer of metal (metal 2) to be stacked on the first (metal 1) (no insulating layer available between), adding about one additional micrometer to the original half-micrometer thickness. While still less than optimal, the thickness of the stacked metal layers brought the peak (2 GHz) Q up from just under five to just over ten, with little effect observed in inductance or SRF. The increase in Q was due in part from reduced ohmic loss, but was also aided by the resulting increase in assembled height caused by the stress of the additional metal. This effect is evident in the two adjacent inductors in Fig. 5. These inductors use a meander shape to increase inductance.

Measurements were also made to assess microphonic and thermal effects on performance; the concern being that any condition that alters the assembled shape could similarly affect the electrical performance. A B&K vibration exciter was used to shake the inductors over a wide frequency range, allowing mechanical resonance to be visually determined under a microscope. Fundamental-mode resonance frequencies ranged from 500 to 1500 Hz, depending on dimensions. For one circular inductor (400-μm-radius 100-μm-width conductors), the measured mechanical resonance was 845 Hz and the full-width-half-maximum was 20 Hz, giving a mechanical Q of about 40. It took 30 g's of acceleration at the resonance frequency to drive the amplitude of motion to one half the original displacement. Cycling the temperature of the inductor environment from extremes of $-50\,^{\circ}$C to $150\,^{\circ}$C, the inductor could clearly be seen to go from a steeply assembled angle to nearly flat on the substrate, respectively. There was little change in inductance below resonance for the two extremes, but Q dropped significantly from about 14 to 6 as the inductor flattened at the maximum temperature. Thermal deformation can also be caused through joule heating from an electrical signal. Passing a dc current of 0.25 A through a typical 400-μm-radius 100-μm-width (metal 1) 2-nH inductor heats it ohmically enough to flatten it. With not too much more current, the conductor melts. The same inductor fabricated with the additional metal 2 can withstand about 0.4 A. These structures have a dc resistance of about 1–2 Ω and, thus, can be thermally flattened with about one-eighth of a watt. Assuming an RF Q of around eight, we can extrapolate an RF power limit of around 1 W [1].

While the effect of thermal deformation was detrimental in the previous example, this same effect was put to use to create Q-stable variable inductors. The performance for the previously described variable inductor is shown in Fig. 3(b). Frequency-swept measurements were made for temperatures ranging from 25 $^{\circ}$C to 200 $^{\circ}$C. At room temperature, the outer loop of the inductor stood at an angle of about 45° and the inner loop was bent even further. As temperature was increased, both loops began to straighten out and flatten toward the substrate at different rates due to different corrugation patterns. In this case, neither loop completely flattened against the substrate, even at 200 $^{\circ}$C. In the vicinity of 4 GHz, Q values remained fairly stable around 5 ($<$10% variation), while inductance values varied from 0.67 to 0.82 nH, greater than 18% (22% referenced to the heated extreme). The values were repeatable as the temperature was cycled. The ambient temperature for the inductors was varied here, but it is also possible to achieve this effect by directly heating only the inductor structure by applying a dc current. Wire loop model simulations for variable inductors using Fasthenry[1] [11] field solver software suggest the range of inductance variation for the two-loop configuration can be enhanced by increasing the coupling between the loops. Fig. 6 illustrates how reducing the gap between inner and outer loops from 25 to 5 μm results in the maximum inductance variation changing from of 27% (37% referred to the alternate extreme) to about 34% (51%), when the angle between the loops varies from 0° to 90°.

In order to further assess fundamental performance limits, electromagnetic simulations were performed using a simple multilayer Sonnet[2] computer-aided design (CAD) model of a square inductor (of similar size to the inductor in Fig. 2) with no anchor pads and a uniform air-gap above the substrate. Parametric variations showed that ohmic losses dominate at the lower frequencies ($<$2 GHz), losses due to the parallel resistance of the mechanical polysilicon layer come into play in the middle frequency range and, above that, the parasitic capacitance between the inductor and substrate ultimately dominates. It was also evident that increasing metal thickness could significantly improve low-frequency Q (to beyond 20 for a 50-μm gap), though the benefits greatly diminish beyond a thickness of about two skin depths (3 μm at 2 GHz). Reducing the local substrate conductivity could further increase the Q beyond 30 for a thin-metal inductor. Examining the gap effect at high frequencies, it was evident that the simple use of the average curved gap size in the uniform gap model was inaccurate and that the anchor pads and slowly tapering rise from the substrate determine the dominant parasitic capacitance [1].

[1]Fasthenry is an inductance extraction program that computes the complex frequency-dependent admittance matrix under the magnetoquasi-static approximation.

[2]Sonnet Software Inc., Liverpool, NY 13088.

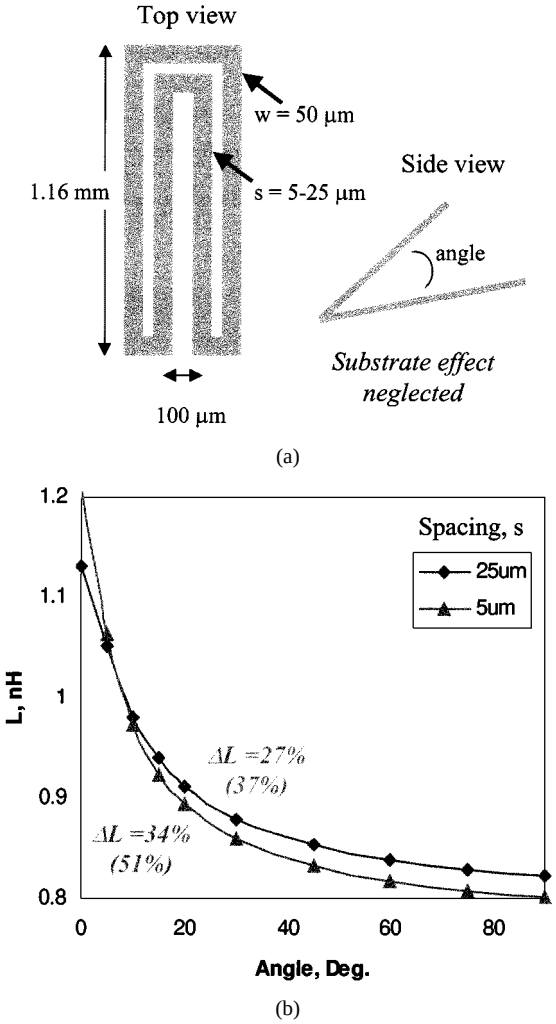

Fig. 6. (a) Hairpin inductor variation with mutual angle. (b) Increasing the mutual coupling between loops by narrowing the gap between them allows for a greater maximum variation in inductance.

These results suggest that thick-metal anchor-pad free designs that rise fast from the substrate should yield the best performance. A comparison of two similar fixed-value inductors illustrating this point is shown in Fig. 4(b). Both were hairpin-shaped with thin metal only, but one was a simple warping structure attached to the substrate with flat anchor pads [similar to the inner loop in Fig. 3(a)], while the other was attached with hinges as previously described. Measured inductance values were very similar for both (about 1 nH), with a slightly higher value for the simple inductor due to the extra length of the anchor pads. At very low frequencies, Q values were similar, as the thin metal was the limiting factor in both cases. At higher frequencies though, the Q value was greatly improved for the hinged inductor, in excess of 13. Furthermore, very little change in inductance was observed for the hinged inductor at varying temperatures. While a simple hairpin design was useful for demonstrating the effect, the absolute performance for this structure was not ideal. Even with only thin metal, wider inductors with a more circular or triangular shape have demonstrated Q values that rise more quickly with frequency and peak at levels greater than twice that of the hairpin, and could be similarly adapted.

IV. Conclusion

High-performance fixed and variable inductors have been demonstrated with Q values in excess of 13 and potentially greater than 20 with additional metal. Most of these inductors can operate up to 20 GHz and beyond. Variable inductors of about 1 nH have been demonstrated with more than 18% variation through thermal control, with variations in excess of 30% predicted for more optimum structures. Fixed inductor designs, with improved temperature-stable Q values, have also been demonstrated. If needed, additional stability could be achieved for the fixed inductors by a final application of a thick dielectric coating, such as polyimide. All inductors were fabricated using common MEMS techniques that are suitable for MEMS-first integration in RFICs and can be useful for applications ranging from device characterization in the laboratory to producing improved performance communications products.

Acknowledgment

The authors wish to thank J. Lin, Lucent Technologies, Murray Hill, NJ, O. Boric-Lubecke, Lucent Technologies, Murray Hill, NJ, V. Aksyuk, Lucent Technologies, Murray Hill, NJ, S. Arney, Lucent Technologies, Murray Hill, NJ, and F. Pardo, Lucent Technologies, Murray Hill, NJ, for useful discussions on RFICs, MEMS, and inductors.

References

[1] P. L. Gammel, B. P. Barber, V. M. Lubecke, N. Belk, and M. R. Frei, "Design, test and simulation of self-assembled, micromachined RF inductors," in *SPIE Design, Test, Microfab. MEMS MOEMS Symp. Dig.*, Mar. 1999, pp. 582–591.

[2] C.-Y. Chi and G. M. Rebiez, "Planar microwave and millimeter-wave lumped elements and coupled-line filters using micromachining techniques," *IEEE Trans. Microwave Theory Tech.*, vol. 43, pp. 730–738, Apr. 1995.

[3] D. J. Young, V. Malba, J.-J. Ou, A. F. Bernhardt, and B. E. Boser, "Monolithic high-performance three-dimensional coil inductors for wireless communication applications," in *IEEE Int. Electron Devices Meeting Tech. Dig.*, Washington, DC, Dec. 8–11, 1997, pp. 67–70.

[4] S. Zhou, X.-Q. Sun, and W. N. Carr, "A monolithic variable inductor network using microrelays with combined thermal and electrostatic actuation," *J. Micromech. Microeng.*, vol. 9, no. 1, pp. 45–50, Mar. 1999.

[5] S. Hara and T. Tokumitsu, "Monolithic microwave active inductors and their applications," in *IEEE Int. Circuits Syst. Symp. Dig.*, June 1991, pp. 1857–1860.

[6] J. Smith, "Embedded micromechanical devices for the monolithic integration of MEMS with CMOS," in *Proc. Int. Electron. Device Meeting*, 1995, pp. 609–612.

[7] W. Cowan, V. Bright, V. A. Elvin, and D. Koester, "Modeling of stress induced curvature in surface micromachined devices," in *SPIE Educ. Program Micromach. Microfab. Symp. Dig.*, 1997, pp. 56–67.

[8] V. Aksyuk, B. P. Barber, C. R. Giles, R. Ruel, L. Stultz, and D. J. Bishop, "Low insertion loss packaged and fiber-connectorized Si surface-micromachined reflective optical switch," in *Proc. Solid-State Sens. Actuator Workshop*, Hilton Head, SC, pp. 79–82.

[9] D. Koester, R. Majedevan, A. Shishkoff, and K. Marcus, "Multi-user MEMS process (MUMPS) introduction and design rules," MCNC (CRONOS) MEMS Technol. Applicat. Center, Research Triangle Park, NC, Rev. 4, July 15, 1996.

[10] V. Lubecke, B. Barber, E. Chan, D. Lopez, and P. Gammel, "Self-assembling MEMS variable and fixed RF inductors," in *Proc. Asia–Pacific Microwave Conf.*, Sydney N.S.W., Australia, Dec. 2000, paper 218, pp. 201–204.

[11] *Fasthenry User's Guide, Ver. 3.0*, Massachusetts Inst. Technol., Cambridge, MA, 1996.

Victor M. Lubecke (S'86–M'86–SM'98) received the B.S. degree in electrical and electronics engineering from the California State Polytechnic University, Pomona, in 1986, and the M.S. and Ph.D. degrees in electrical engineering from the California Institute of Technology, Pasadena, in 1990 and 1995, respectively. His graduate work focused on the development of MEMS techniques for terahertz ICs.

From 1987 to 1996, he was a Member of the Technical Staff at the NASA Jet Propulsion Laboratory. From 1996 to 1998, he was a Visiting Researcher at the Photodynamics Research Center, The Institute for Physical and Chemical Research (RIKEN), Sendai, Japan. His work has involved the investigation and development of millimeter- and submillimeter-wave technology for space communications and remote-sensing applications. Since 1998, he has been a Member of the Technical Staff at Bell Laboratories, Lucent Technologies, Murray Hill, NJ. His current research interests include wireless circuits and applications, MEMS techniques, and biomedical technology.

Bradley Barber (M'98) was born in Oakridge, TN, in 1965. He received the Ph.D. degree in physics (specifically physical acoustics) from the University of California at Los Angeles (UCLA), in 1992.

In 1995, he joined AT&T Bell Laboratories, Murray Hill, NJ, as a Post-Doctoral Researcher, where he was involved with photostrictive ceramics and superconductivity. Since becoming a Member of Technical Staff at Bell Laboratories in 1997 (then part of Lucent Technologies), his research has focused on improving performance of RF passives, especially novel MEMS and acoustic-wave-based devices. He is currently a Technical Manager with Agere Systems (formerly the Microelectronics Group, Lucent Technologies), Murray Hill, NJ, where he supervises research toward integrating high-performance RF passives, and nonstandard processing improvements of RF circuits.

Edward Chan, photograph and biography not available at time of publication.

Daniel Lopez, photograph and biography not available at time of publication.

Mihal E. Gross received the B.Sc. degree in chemistry from the Massachusetts Institute of Technology (MIT), Cambridge, in 1977, and M.Sc. and Ph.D. degrees in chemistry from Northwestern University, Evanston, IL, in 1978 and 1981, respectively.

In 1981, she joined the Physical Sciences Research Division, Bell Laboratories, Murray Hill, NJ, as a Member of Technical Staff, and is currently in the Electronic Devices Research Laboratory, Agere Systems (formerly the Microelectronics Group, Lucent Technologies), Murray Hill, NJ. Her current research is focused on materials and integration issues and metallization for RF and optical MEMS devices. This follows her studies into the mechanism of room-temperature recrystallization of electroplated Cu and its ramifications for dual damascene Cu interconnects. Her research activities have also included laser and ion beam direct-write, thermal and plasma-enhanced chemical vapor deposition, and spin-on metal–organic fabrication of high Tc superconductor thin films.

Peter Gammel (M'00), photograph and biography not available at time of publication.